

REPORT DOCUMENTATION PAGE				Form Approved OMB No. 0704-0188	
The public reporting burden for this collection of information is estimated to average 1 hour per response, including the time for reviewing instructions, searching existing data sources, gathering and maintaining the data needed, and completing and reviewing the collection of information. Send comments regarding this burden estimate or any other aspect of this collection of information, including suggestions for reducing the burden, to the Department of Defense, Executive Services and Communications Directorate (0704-0188). Respondents should be aware that notwithstanding any other provision of law, no person shall be subject to any penalty for failing to comply with a collection of information if it does not display a currently valid OMB control number.					
PLEASE DO NOT RETURN YOUR FORM TO THE ABOVE ORGANIZATION.					
1. REPORT DATE (DD-MM-YYYY) 14-01-2010		2. REPORT TYPE Conference Proceeding		3. DATES COVERED (From - To)	
4. TITLE AND SUBTITLE Spectral Variability of Airborne Ocean Color Data Linked to Variations in Lidar Backscattering Profiles				5a. CONTRACT NUMBER	
				5b. GRANT NUMBER	
				5c. PROGRAM ELEMENT NUMBER 0601153N	
				5d. PROJECT NUMBER	
6. AUTHOR(S) M.A. Montes-Hugo, Richard Gould, Z. Lee, R. Arnone, D. Gray, J. Churnside				5e. TASK NUMBER	
				5f. WORK UNIT NUMBER 73-9857-09-5	
7. PERFORMING ORGANIZATION NAME(S) AND ADDRESS(ES) Naval Research Laboratory Oceanography Division Stennis Space Center, MS 39529-5004				8. PERFORMING ORGANIZATION REPORT NUMBER NRL/PP/7320-09-9294	
9. SPONSORING/MONITORING AGENCY NAME(S) AND ADDRESS(ES) Office of Naval Research 800 N. Quincy St. Arlington, VA 22217-5660				10. SPONSOR/MONITOR'S ACRONYM(S) ONR	
				11. SPONSOR/MONITOR'S REPORT NUMBER(S)	
12. DISTRIBUTION/AVAILABILITY STATEMENT Approved for public release, distribution is unlimited.					
20100121304					
13. SUPPLEMENTARY NOTES					
14. ABSTRACT Characterization of 3-D underwater light fields from above the sea surface requires passive and active remote sensing measurements. In this work, we suggest the use of passive ocean color sensors and lidar (Light Detection and Ranging) to examine the vertical structure of optical properties in marine waters of the Northern Part of the Gulf of Alaska (NGOA). We collected simultaneous airborne remote sensing reflectance (R_{rs}) in the spectral range 443-780 nm (MicroSAS, Satlantic) and lidar-derived volume backscattering profiles (0-20 m depth, wavelength = 532 nm) during August 17 2002 in shelf waters situated south of Kodiak Island off Alaska (57.48°-58.04° N, 152.91°-151.67° W). We evaluated the spectral response of R_{rs} to perturbations on vertical distribution of by comparing the spatial variability between aggregated (250 m horizontal resolution x 1 m vertical resolution) R_{rs} spectral ratios and different lidar statistics per bin (Maximum per bin, mean per bin, σ , standard deviation of per bin, integrated per bin, μ) or group of bins (lidar volume extinction coefficient of between 0 and 5 m depth). Sub-surface changes of μ , σ , and μ_{int} were mainly correlated with R_{rs} (490)/ R_{rs} (555) variability along the flight-track (Semi-partial correlation coefficients = 0.12 to 0.21). Our results evidenced linkages between above and below-sea surface optical properties that can be used to derive water optical constituents as a function of depth based on combined passive-active data.					
15. SUBJECT TERMS gliders, ocean color sensors, data fusion, remote sensing reflectance, particle size distribution, vertical structure, optical properties					
16. SECURITY CLASSIFICATION OF:			17. LIMITATION OF ABSTRACT UL	18. NUMBER OF PAGES 9	19a. NAME OF RESPONSIBLE PERSON Richard Gould
a. REPORT Unclassified	b. ABSTRACT Unclassified	c. THIS PAGE Unclassified			19b. TELEPHONE NUMBER (Include area code) 228-688-5587

PUBLICATION OR PRESENTATION RELEASE REQUEST

Pubkey: 6228

NRLINST 5600.2

1. REFERENCES AND ENCLOSURES	2. TYPE OF PUBLICATION OR PRESENTATION	3. ADMINISTRATIVE INFORMATION
Ref: (a) NRL Instruction 5600.2 (b) NRL Instruction 5510.40D Encl: (1) Two copies of subject paper (or abstract)	<input type="checkbox"/> Abstract only, published <input type="checkbox"/> Book <input type="checkbox"/> Conference Proceedings (refereed) <input type="checkbox"/> Invited speaker <input type="checkbox"/> Journal article (refereed) <input type="checkbox"/> Oral Presentation, published <input type="checkbox"/> Other, explain	<input type="checkbox"/> Abstract only, not published <input type="checkbox"/> Book chapter <input checked="" type="checkbox"/> Conference Proceedings (not refereed) <input type="checkbox"/> Multimedia report <input type="checkbox"/> Journal article (not refereed) <input type="checkbox"/> Oral Presentation, not published
		STRN NRL 7330-09-9294 Route Sheet No. 7330/ Job Order No. 73-9857-09-5 Classification <input checked="" type="checkbox"/> X <input type="checkbox"/> U <input type="checkbox"/> C Sponsor ONR approval obtained <input type="checkbox"/> yes <input checked="" type="checkbox"/> no

4. AUTHOR

Title of Paper or Presentation

Spectral Variability of Airborne Ocean Color Data Linked to Variations in Lidar Backscattering Profiles

Author(s) Name(s) (First, MI, Last), Code, Affiliation if not NRL

M.A. Montes- Hugo, Richard W. Gould, ZhongPing Lee, Robert A Arnone, Deric Gray, J. Churnside

It is intended to offer this paper to the **SPIE Optics & Photonics 2009 Meeting**

(Name of Conference)

02- AUG - 06- AUG- 09, San Diego, CA, Unclassified

(Date, Place and Classification of Conference)

and/or for publication in **SPIE Optics & Photonics 2009 Meeting, Unclassified**

(Name and Classification of Publication)

(Name of Publisher)

After presentation or publication, pertinent publication/presentation data will be entered in the publications data base, in accordance with reference (a).

It is the opinion of the author that the subject paper (is ☐) (is not ☒) classified, in accordance with reference (b).

This paper does not violate any disclosure of trade secrets or suggestions of outside individuals or concerns which have been communicated to the Laboratory in confidence. This paper (does ☐) (does not ☒) contain any militarily critical technology.

This subject paper (has ☐) (has never ☒) been incorporated in an official NRL Report.

Richard W. Gould, 7333

Name and Code (Principal Author)

(Signature)

5. ROUTING/APPROVAL

CODE	SIGNATURE	DATE	COMMENTS
Author(s) <i>Gould</i>	<i>RW Gould</i>	<i>7/14/09</i>	Need by <u><i>31 Jul 09</i></u> Publicly accessible sources used for this publication
Section Head <i>N/A</i>			
Branch Head Robert A Arnone, 7330	<i>R Arnone</i>	<i>7/14/09</i>	
Division Head Ruth H. Preller, 7300	<i>Ruth H. Preller</i>	<i>7/15/09</i>	1. Release of this paper is approved. 2. To the best knowledge of this Division, the subject matter of this paper (has <input type="checkbox"/>) (has never <input checked="" type="checkbox"/>) been classified.
Security, Code 1226			1. Paper or abstract was released. 2. A copy is filed in this office. <i>950-253-9</i>
Office of Counsel, Code 1008.3			
ADOR/Director NCST E. R. Franchi, 7000			
Public Affairs (Unclassified/ Unlimited Only), Code 7030.4	<i>Shannon Franchi</i>	<i>7/25/09</i>	
Division, Code			
Author, Code			

PUBLICATION OR PRESENTATION RELEASE REQUEST

Pub

623

NRL INST 5800.2

09. 1226 2499

1. REFERENCES AND ENCLOSURES		2. TYPE OF PUBLICATION OR PRESENTATION		3. ADMINISTRATIVE INFORMATION	
Ref: (a) NRL Instruction 5800.2 (b) NRL Instruction 5510.40D	<input type="checkbox"/> Abstract only, published <input type="checkbox"/> Book <input type="checkbox"/> Conference Proceedings (referenced) <input type="checkbox"/> Invited speaker <input type="checkbox"/> Journal article (referenced) <input type="checkbox"/> Oral Presentation, published <input type="checkbox"/> Other, explain	<input type="checkbox"/> Abstract only, not published <input type="checkbox"/> Book chapter <input checked="" type="checkbox"/> Conference Proceedings (not referenced) <input type="checkbox"/> Multimedia report <input type="checkbox"/> Journal article (not referenced) <input type="checkbox"/> Oral Presentation, not published	STRN: <u>NRL 097330-09-9294</u> Route Sheet No. <u>7330/</u> Job Order No. <u>73-9857-09-5</u> Classification <input checked="" type="checkbox"/> U <input type="checkbox"/> C Sponsor <u>ONR</u> approval obtained <u>yes</u> <input checked="" type="checkbox"/> no		
4. AUTHOR					
Title of Paper or Presentation <u>Spectral Variability of Airborne Ocean Color Data Linked to Variations in Lidar Backscattering Profiles</u>					
Author(s) Name(s) (First, M./Last), Code, Affiliation if not NRL <u>M.A. Montes-Hugo, Richard W. Gould, ZhongPing Lee, Robert A. Amone, Deric Gray, J. Churnside</u>					
It is intended to offer this paper to the <u>SPIE Optics & Photonics 2009 Meeting</u> (Name of Conference) <u>02-AUG - 06-AUG-09, San Diego, CA, Unclassified</u> (Date, Place and Classification of Conference)					
and/or for publication in <u>SPIE Optics & Photonics 2009 Meeting, Unclassified</u> (Name and Classification of Publication)					
After presentation or publication, pertinent publication/presentation data will be entered in the publications data base, in accordance with reference (a). It is the opinion of the author that the subject paper (is <u> </u>) (is not <u>X</u>) classified, in accordance with reference (b). This paper does not violate any disclosure of trade secrets or suggestions of outside individuals or concerns which have been communicated to the Laboratory in confidence. This paper (does <u> </u>) (does not <u>X</u>) contain any militarily critical technology. This subject paper (has <u> </u>) (has never <u>X</u>) been incorporated in an official NRL Report.					
Richard W. Gould, 7333 (Name and Code (Principal Author)) <u>RWGould</u> (Signature)					
5. ROUTING APPROVAL					
CODE	SIGNATURE	DATE	COMMENTS		
Author(s) <u>Gould</u>	<u>RWGould</u>	<u>7/14/09</u>	Need by <u>31 Jul 09</u> Publicly accessible sources used for this publication		
Section Head <u>N/A</u>			This is a Final Security Review. Any changes made in the document after approved by Code 1226 nullify the Security Review		
Branch Head <u>Robert A. Amone, 7330</u>	<u>R. Amone</u>	<u>7/14/09</u>	1. Release of this paper is approved. 2. To the best knowledge of this Division, the subject matter of this paper (has <u> </u>) (has never <u>X</u>) been classified.		
Division Head <u>Ruth H. Preller, 7300</u>	<u>Ruth H. Preller</u>	<u>7/15/09</u>	1. Paper or abstract was released. 2. A copy is filed in this office. <u>SSC-253-9</u>		
Security Code <u>1226</u>	<u>David A. Uccella</u>	<u>7/20/09</u>	Sponsor <u>Approved Attached</u>		
Office of Counsel Code <u>1008.3</u>					
ADOR/Director NCST <u>E. R. Franchi, 7000</u>					
Public Affairs (Unclassified/Unlimited Only) Code <u>7030.4</u>	<u>Shirley R. Franchi</u>	<u>7/22/09</u>			
Division Code					
Author Code					

Spectral variability of airborne ocean color data linked to variations in lidar backscattering profiles

Montes-Hugo M.A.^{1,2*}, Gould R.², Lee Z.¹, Arnone R.², Gray D.³, Churnside J.⁴

¹Northern Gulf Institute, Mississippi State University, MS 39529, USA; *E-mail: mam813@msstate.edu

²Naval Research Lab, Stennis Space Center, NASA, MS 39529, USA

³Naval Research Lab, Washington DC, 20375, USA

⁴NOAA Earth System Research Laboratory, CO 80305 USA

ABSTRACT

Characterization of 3-D underwater light fields from above the sea surface requires passive and active remote sensing measurements. In this work, we suggest the use of passive ocean color sensors and lidar (Light Detection and Ranging) to examine the vertical structure of optical properties in marine waters of the Northern Part of the Gulf of Alaska (NGOA). We collected simultaneous airborne remote sensing reflectance (R_{rs}) in the spectral range 443-780 nm (MicroSAS, Satlantic) and lidar-derived volume backscattering (β) profiles (0-20 m depth, wavelength = 532 nm) during August 17 2002 in shelf waters situated south of Kodiak Island off Alaska (57.48°-58.04° N, 152.91°-151.67° W). We evaluated the spectral response of R_{rs} to perturbations on vertical distribution of β by comparing the spatial variability between aggregated (250 m horizontal resolution x 1 m vertical resolution) R_{rs} spectral ratios and different lidar statistics per bin (Maximum β per bin, mean β per bin, β_m , standard deviation of β per bin, β_{std} , integrated β per bin, β_{int}) or group of bins (lidar volume extinction coefficient of β between 0 and 5 m depth). Sub-surface changes of β_m , β_{int} , and β_{std} were mainly correlated with $R_{rs}(490)/R_{rs}(555)$ variability along the flight-track (Semi-partial correlation coefficients = 0.12 to 0.21). Our results evidenced linkages between above and below-sea surface optical properties that can be used to derive water optical constituents as a function of depth based on combined passive-active data.

Keywords: lidar, ocean color sensors, water visibility, visible spectrum, active sensors, remote sensing, vertical structure, underwater light field models

1. INTRODUCTION

Passive and active optical remote sensing systems have inherent limitations for reconstructing optical light fields within the upper oceanic layers (~0-30 m depth). Inherent and apparent optical properties in the first optical depth (~20 m = $1/K_d$, where K_d is the vertically diffuse attenuation coefficient for downwelling light) can be derived from inversion of above-water remote-sensing reflectance ($R_{rs}(\lambda, 0_+)$) (spectral range = 400-700 nm) measurements obtained by passive spectrometers¹. If time and geographic location are unchanged, variability of $R_{rs}(\lambda, 0_+)$ is related to concentration of different optically-active compounds (particulate and dissolved) and vertical distribution of those components^{2,3}. In other words, ocean color observations from airborne or satellite passive sensors offer a vertically-integrated view of optical constituents through the water column and may not be able to discriminate depth-related optical features such as thin layers⁴.

In contrast to passive remote sensing technologies, active sensors such as lidar (Light detection and Ranging), can obtain optical measurements deeper than one optical depth and can resolve vertical differences on signal strength by using short laser pulses coupled with high speed time-gated detectors⁵. Typical lidar systems used from airplanes (e.g., FLOE, fluorescence)^{6,7} and satellites (e.g. CALIPSO)⁸ have fewer wavelengths compared to ocean color passive sensors, one or two in the visible (e.g., excitation wavelength in FLUOR is 432 nm) and one in the IR (e.g., 1100 nm) spectrum. This spectral paucity represents a constraint to discriminate targets with distinct absorption and scattering signatures. Also, differentiation of optical components is challenging when lidar measurements (e.g., FLOE) are based on backscattering

since the relatively wide dynamic range of backscattering strength, and consequently possible optical identities⁶. The inclusion of polarizers prior to detection has been an alternative to minimize the spectral limitations of some lidar sensors (e.g., analysis of depolarization ratios using CALIPSO profiles)⁹.

In the present study we evaluate the potential use of concurrent passive and active optical measurements to retrieve the vertical profile 'shape' of inherent optical properties (IOPs) in shelf waters of the northern part of the Gulf of Alaska (NGOA). Spatial patterns of ocean color and lidar measurements are expected to be linked due to changes on backscattered photons at green wavelengths. We present preliminary results showing how different lidar-backscattering parameters are related to $R_{rs}(\lambda, 0_+)$ spectral variability based on aerial surveys performed during summer and when oceanographic conditions favor the formation of diverse planktonic layers in the euphotic zone (0-50 m depth).

2. METHODS

2.1 Aerial surveys and flight mission settings

Airborne spectral upwelling radiances (L_u) and downwelling irradiance (E_d) in the visible spectral range (400–700 nm), and lidar backscattering (β) data (green laser at 532 nm) were gathered over waters of the eastern shelf of Afognak/Kodiak Islands (57.48°–58.04° N, 152.91°–151.67° W) during August 17 of 2002 (Fig. 1).

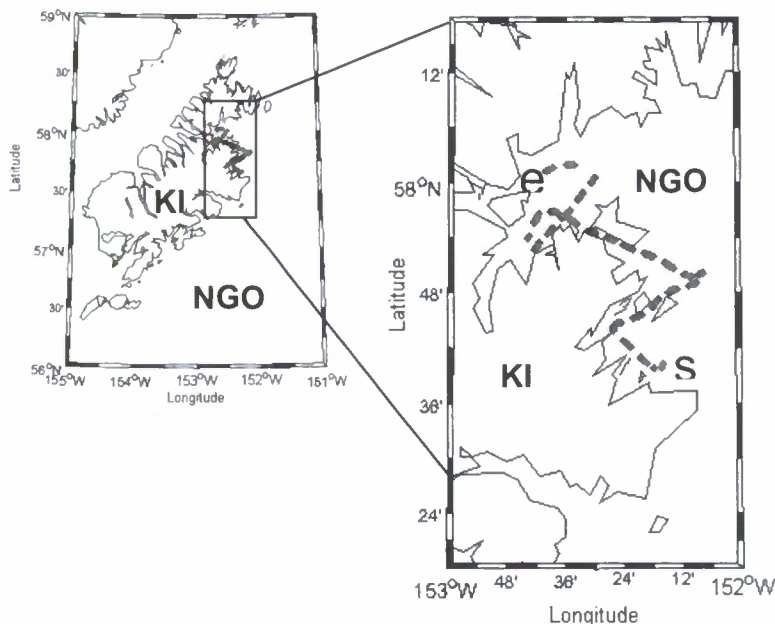


Fig. 1. Aerial survey over the NGOA shelf. Start (s) and end (e) locations during August 17, 2002 flight mission are indicated. KI: Kodiak Island, NGOA: Northern Part of the Gulf of the Alaska. The full dataset of remote sensing measurements was obtained between 12:54 and 13:22 pm local time and over waters deeper (>50 m depth) than penetration depth of the lidar system.

Optimal flight weather conditions (i.e., cloud-free skies, wind speed $< 4 \text{ m s}^{-1}$) were checked a priori to maximize the number of comparisons between passive and active optical measurements. For the whole aerial survey, the flying altitude and speed was standardized at 305 m and 247 km h^{-1} , respectively. Based on these average flight characteristics, we collected 10^4 passive radiometric measurements (upwelling and downwelling) and $5.6 \cdot 10^4$ lidar shots along a total distance of 108 km and during 28 minutes. MicroSAS and lidar data were geo-located every 1 minute during the full survey.

2.2 Passive optical measurements

2.2.1 Optical sensors

Measurements of L_u and E_d were performed at 411, 443, 491, 509, 553, 665, and 780 nm (10 nm bandwidth) with a spectrometric Micro Surface Acquisition System (MicroSAS). These wavelengths were designed to match spaceborne ocean color sensors such as SeaWiFS. MicroSAS has two digital optical sensors (L : OCR-507-R03A, E_d : OCR-507-ICSA, Satlantic inc., Canada). As specified by the manufacturer, field-of-view of the upwelling radiance sensor is 28° in air, and has a typical saturation of $5 \mu\text{Wcm}^{-2} \text{nm}^{-1}$. Based on this FOV and a sampling rate of 360 observations per minute, typical pixel size of L_u MicroSAS measurements was 11.5 m (along-track) by 200 m (across-track). Downwelling irradiance data were used to discriminate cloudy patches and calculate $R_{rs}(\lambda, 0_+)$ in each location. The irradiance sensor has a typical saturation of $300 \mu\text{Wcm}^{-2} \text{nm}^{-1}$ and a noise equivalent of $2.510^3 \mu\text{Wcm}^{-2} \text{nm}^{-1}$.

2.2.2 Atmospheric corrections

A quasi-singlc-scattering approximation was suggested (Rayleigh-aerosol multiple scattering ignored) to relate water-leaving radiance (L_w) to L_u ¹⁰:

$$L_u(\lambda) = L_r(\lambda) + L_a + t(\lambda) L_w(\lambda) + L_{glint} \quad (1)$$

where $t(\lambda)$ is diffuse transmittance of the atmosphere, L_r , L_a and L_{glint} are radiance contributions due to Rayleigh, aerosol, and glint, respectively. L_r is derived from radiance phase functions for water molecules that depend on incident solar angles (zenith and azimuth), and Fresnel reflectance estimates. L_a was calculated over clearwater pixels where a minimum water-leaving radiance at 665 nm is expected ($L_a = k \{L_t(665) - L_r(665)\}$, where k is a constant assuming a maritime atmosphere)¹⁰. L_{glint} was quantified with a first-order adjustment by subtracting $L_t(780)$ to L_t ¹¹. Skylight path radiance contribution was assumed small due to the relatively thin atmospheric layer between the airplane and the sea surface. Further details about atmospheric corrections are described in a previous work¹². Assuming a negligible attenuation of E_d due to the atmospheric path below the airplane, the remote sensing reflectance above the sea-surface ($R_{rs}(\lambda, 0_+)$) was derived as normalized water leaving radiance ($nL_w(\lambda, 0_+)$) divided by $E_d(\lambda, 0_+)$.

In case 1 waters, $R_{rs}(\lambda, 0_+)$ can be approximately related ($\sim 20\%$ bias) to inherent optical properties of the water body with the following expression¹³:

$$R_{rs}(\lambda, 0_+) \approx 0.54 R/Q \quad (2)$$

$$R/Q = 0.095 \{b_b(\lambda)/(b_b(\lambda) + a(\lambda))\} \quad (3)$$

where b_b is the total backscattering coefficient (water + particulates), a is the total absorption coefficient of water including colored dissolved organic matter and particulates and R/Q is a shape distribution factor that is influenced by the light field geometry.

2.3 Active optical measurements

Lidar backscattering measurements were obtained with a Fish Lidar Oceanic Experimental (FLOE) system¹⁴ mounted downwards from the port side of a twin-engine aircraft. FLOE was set up 15° off vertical to minimize specular reflections from the sea. For each lidar pulse, β_t or the sum of water (β_w) and particulate (i.e., phytoplankton, zooplankton, fish) (β_p) contributions was computed from photocathode current measurements (S) as a function of depth (z):

$$S(z) = A \beta_t(z) (L(z)^{-2}) e^{-2\alpha z} + B \quad (4)$$

where A is an amplitude parameter that depends on the optical system parameters and the geometry (e.g., laser pulse energy, surface losses, receiver area, detector responsivity), L is the optical distance from the aircraft to the measurement depth in m, α is the lidar attenuation coefficient in m^{-1} , B is the background signal level coming from skylight contribution. The quantities $A\beta_w$ and α were found for each lidar pulse based on equation (4) and

assuming that β_w does not vary with depth, and β_p is zero at a depth of 2 m and at the maximum penetration depth of each lidar pulse (i.e., $S(z)$ above 10 standard deviations of receiver noise).

For most of the surveyed area, FLOE yielded a total of 2,000 lidar shots (i.e., profiles) per minute or 1 'scene' in about 4.1 km distance. This corresponds with a laser sampling rate of 30 Hz and results in a pixel size of circa 2 m (along-track) by 5 m (across-track) by 0.1 m (along the vertical). The laser is linearly polarized and has beam divergence of 50 mrad during daylight hours that allow β measurements as deep as 100 m. However, due to the background absorption of laser energy with depth, FLOE penetration depth in our study area was 30 m depth in average or 10^{-9} A in terms of photocathode current. The green laser source was pulsed with energy of 100 mJ and a length of 15 nsec. The FLOE detector has a cross-polarizer in front of the telescope to maximizing contrast between fish and smaller light-scattering particles¹⁵.

2.4 Calculation of remote sensing products

To examine relationships between above-water remote sensing reflectance and lidar backscattering measurements we calculated six variables based on MicroSAS data (5 spectral band ratios, $R_{rs}(410)/R_{rs}(555)$, $R_{rs}(443)/R_{rs}(555)$, $R_{rs}(490)/R_{rs}(555)$, $R_{rs}(508)/R_{rs}(555)$, $R_{rs}(443)/R_{rs}(490)$, and 1 spectral curvature ratio, $G(1,1) = R_{rs}(490)^2/\{R_{rs}(443)R_{rs}(508)\}$), and five variables based on FLOE-derived β measurements per bin (Maximum β per bin, β_{max} , mean β per bin, β_m , standard deviation of β per bin, β_{std} , integrated β per bin, β_{int}) and group of vertical bins (lidar volume extinction coefficient of β between 0 and 5 m depth, α_β). Notice that using R_{rs} ratios allow MicroSAS-FLOE comparisons to be almost independent on sunlight illumination conditions. Likewise, the use of different R_{rs} wavelengths may help to interpret the nature of optical particulate components determining β (e.g., $R_{rs}(443)/R_{rs}(490)$ is sensitive to particle size distribution)¹⁶.

2.5 Statistical analysis

Spatial coherence between passive and active optical measurements was quantified using multiple regression analysis where the independent variable was one of the proposed spectral R_{rs} ratios, and the dependent variables were the β -derived parameters calculated at different depths.

Before each run, R_{rs} and β parameters were aggregated (MicroSAS data in 250-m (along-track), FLOE data in 250-m (along-track) by 1 m (along the vertical)) in bins. The choice of 250-m spatial resolution in the horizontal component coincides with the maximum spatial resolution provided by some global ocean color sensors (e.g., MODIS). Also, this resolution roughly matches the swath of MicroSAS radiometric measurements in the visible range (across-track pixel size = 200 m). Intensity of covariation between MicroSAS and FLOE variables was measured based on semi-partial correlation coefficients (ρ). Relative contribution of each depth to spatial changes on R_{rs} ratios was estimated by comparing magnitude of ρ of only those depths with significant coefficients at 95% of confidence level.

3. RESULTS AND DISCUSSION

The simultaneous use of passive ocean color measurements and lidar profiles put in evidence spatial relationships between R_{rs} ratios and β -derived quantities for a broad range of spatial scales varying between 250-m and 50 km along the flight direction (Fig. 2, Table 1).

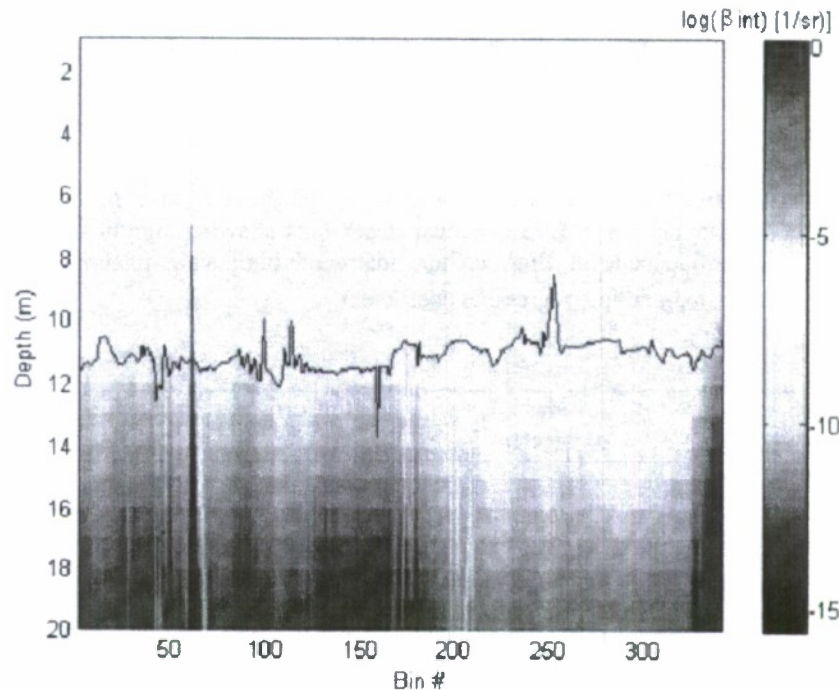


Fig. 2 An example of lidargram during August 17, 2002 survey over coastal waters of Kodiak Island. The whole section encompasses 108 km of horizontal distance or 28 minutes of flight duration. Vertically and horizontally integrated lidar volume-backscattering (β_{int}) is plotted in \log_{10} scale as a function of depth. Spatial integration of β_{int} consisted in size bins of 250 m (horizontal) by 1 meter (vertical). $R_{rs}(490, 0_+)/R_{rs}(553, 0_+)$ is depicted with a solid line and relative units. Remote sensing reflectance ratio spikes in along-track bins # 100, 110 and 250 were related to patchy distribution of low clouds (i.e., drops on downwelling irradiance at 780 nm). This effect was amplified in those R_{rs} ratios based on shorter wavelengths in the numerator.

In Figure 2, we show the best spatial coherence, in terms of ρ , between passive and active optical measurements performed from a low altitude aircraft. β_{int} and $R_{rs}(490, 0_+)/R_{rs}(553, 0_+)$ values were positively correlated, and that correlation was greater in the first meters of the water column (Table 1). Also, spatial variability (magnitude) of MicroSAS R_{rs} ratios tended to be higher (lower) for locations where β_{int} decreased drastically with depth and especially beyond 10 m (e.g., bin # 1 to 175). Assuming minor surface effects (glint, bubbles and foam), the intensification of lidar returns near the sea surface was likely caused by greater concentrations of phytoplankton and relatively small (≤ 250 m) fish schools. Surfacing of zooplankton due to upward migration was unlikely during the sampling period since these organisms start moving toward the sea surface at the end of the evening twilight (sunset 20:05 h, local time in Kodiak Island during August 17, 2002). The elevated $R_{rs}(490, 0_+)/R_{rs}(553, 0_+)$ associated with relatively high β_{int} is less straightforward to explain due to the lack of concurrent *in situ* biological data. At a wavelength of 532 nm, zooplankton and fish have a stronger interaction with the lidar waveform in terms of backscattering (i.e., more reflective targets) compared to phytoplankton cells. Likewise, absorption of blue wavelengths (450-495 nm) due to phytoplankton photosynthetic pigments and colored dissolved organic matter is a major light attenuation process compared those contributions originated from fish or zooplankton. Since $R_{rs}(553, 0_+)$ was relatively constant between bin numbers 1-175 and 175-345 (Fig. 3, upper curve), the main change on $R_{rs}(490, 0_+)/R_{rs}(553, 0_+)$ was mainly determined by blue light attenuation differences. Given that fish reflectivity in the blue is relatively low¹⁷, the increase of $R_{rs}(490, 0_+)$ relative to $R_{rs}(553, 0_+)$ for higher β_{int} values was probably attributed to lower phytoplankton concentrations (less light absorption at 490 nm) and greater zooplankton densities (greater retro-scattering of photons at 532 nm). Based on daily FLOE

measurements, integrated β over the upper 20 m and averaged over a distance of 2.5 km has been shown to be positively related to zooplankton settled volume during the same month of 2000¹⁸.

Table 1. Statistical relationships between above-water remote sensing reflectance ratios and under-water lidar parameters. In all cases, comparisons between optical measurements were performed with 250-m horizontal resolution (MicroSAS and FLOE) by 1 meter vertical resolution (FLOE) bins.

β_m : arithmetic average of lidar-derived volume backscattering (β) per bin ($\text{sr}^{-1} \text{m}^{-1}$), β_{std} : standard deviation of β per bin ($\text{sr}^{-1} \text{m}^{-1}$), β_{int} : integrated β per bin (m^{-1}), BinCorr: lidar depth bins showing significant semi-partial correlation with spectral band ratio at 95% confidence level, BinMaxCorr: lidar depth bin having maximum semi-partial correlation with spectral band ratio, r^2_{adj} : adjusted multiple regression coefficient.

MicroSAS spectral ratio ^a	Lidar parameter	BinCorr (m)	BinMaxCorr (m)	r^2_{adj}
1	β_{std}	1,2,7,8,12	8	0.19
2	β_m	1,5,6,13	1	0.41
	β_{std}	1,2,7,8,14	1	0.35
	β_{int}	1	1	0.44
3	β_m	1	1	0.35
	β_{std}	1,2,8,14	1	0.31
	β_{int}	1,3,4,5	1	0.41
4	β_m	1	1	0.24
	β_{std}	1,13	1	0.18
	β_{int}	1,20	1	0.26

^aSpectral band ratio 1: $R_{rs}(443, 0_+)/R_{rs}(553, 0_+)$, 2: $R_{rs}(490, 0_+)/R_{rs}(553, 0_+)$, 3: $R_{rs}(508, 0_+)/R_{rs}(553, 0_+)$, and 4: $R_{rs}(443, 0_+)/R_{rs}(490, 0_+)$.

Unlike band spectral ratios, spatial variability of spectral curvature ratios was not related to horizontal variability of lidar parameters. In general, G (1, 1) variations reflect change on scattering versus absorption properties of phytoplankton communities as phytoplankton blooms develop¹². However, the weak connection between G and lidar-backscattering parameters was more likely related to variability of R_{rs} at 443 nm in G denominator caused by changes on sea surface roughness. The same reason may explain the poorer relationship of β_{int} , β_m and β_{std} with $R_{rs}(443, 0_+)/R_{rs}(553, 0_+)$ and $R_{rs}(443, 0_+)/R_{rs}(490, 0_+)$ (Table 1). Lidar-based parameters such as β_{max} were also highly influenced by wind and wave effects near the sea surface becoming a variable hard to predict based on above-water water leaving radiance ratios.

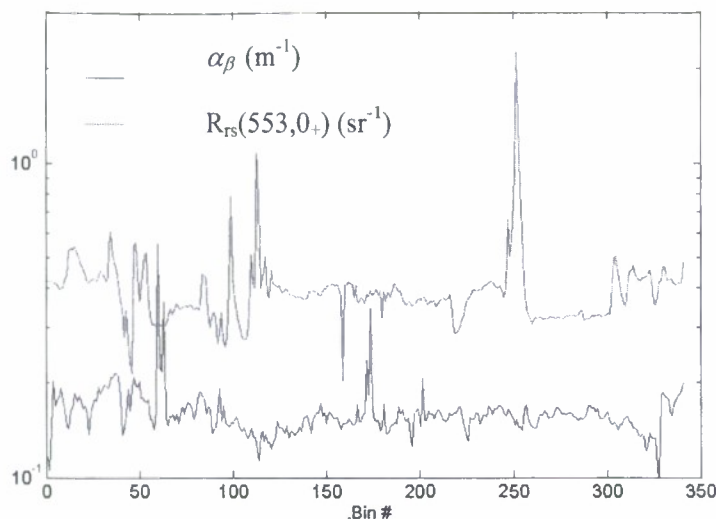


Fig. 3. Spatial variability of passive and active remote sensing variables that link above and in-water optical properties. In left-y axis and logarithm scale with base 10, $R_{rs}(553, 0_+)$: above-water remote sensing reflectance derived from MicroSAS at a wavelength of 553 nm (sr^{-1}) (upper curve), α_β : lidar attenuation coefficient of β calculated within the first five meters of the water column (m^{-1}) (lower curve).

In general for the spectral range 443-508 nm, spatial changes on R_{rs} band ratios had a greater association with β_{int} than with β_m , suggesting a primary influence of number of particles including aggregates with respect to particle composition modulating horizontal patterns of R_{rs} and β (Table 1, Fig. 4A,C). With the exception of $R_{rs}(443, 0_+)/R_{rs}(490, 0_+)$ comparisons, the maximum depth at which lidar parameters still have significant covariability with surface R_{rs} ratios was commonly greater for β_{std} with respect to β_{int} and β_m (Fig. 4A,C-D). This should not be surprising since β_{std} had generally a smaller vertical variation compared to β_{max} , β_{int} , or β_m , thus a shorter decorrelation length scale as a function of depth is expected between MicroSAS-derived R_{rs} ratios and lidar parameters related with abundance or type of optical backscattering components (Fig. 4D). In general, along-track variability of R_{rs} band ratios was quite indifferent to horizontal changes on α_β (Fig. 3, lower curve). This may likely related to a weaker influence of vertical distribution of scatterers compared to their abundance and type on R_{rs} ratios between lidar shots and for β measured within 0-5 depth.

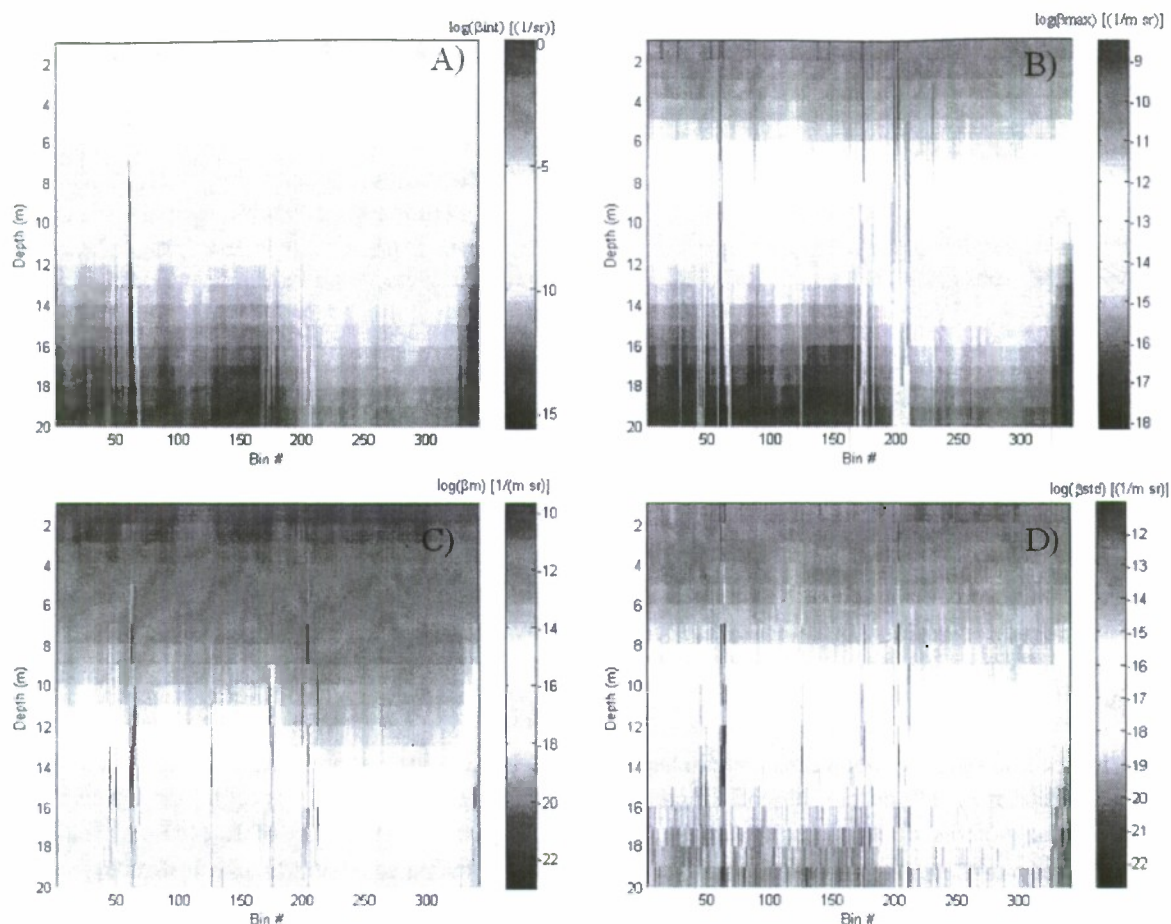


Fig. 4. Vertical cross-section of lidar-derived parameters during the aerial survey made in August 17, 2002. In \log_{10} scale, A) Vertically integrated volume backscattering, β_{int} (sr^{-1}), B) Maximum volume backscattering per bin, β_{max} ($\text{m}^{-1} \text{sr}^{-1}$), C) Mean volume backscattering per bin, β_m ($\text{m}^{-1} \text{sr}^{-1}$), D) Standard deviation of volume backscattering per bin, β_{std} ($\text{m}^{-1} \text{sr}^{-1}$). Each bin represents 250 m along the flight direction and 1 m section as a function of water depth.

Interpretation of functionalities between R_{rs} ratios and β spatial variability is a challenging topic due mainly to two reasons. Firstly, even using the same wavelength, the origin of photons measured by MicroSAS (first optical depth) and lidar (0-30 m depth every 0.1 m) sensors is different, and secondly, β is more influenced by relatively 'large' targets (e.g. zooplankton, fish) with respect to R_{rs} (e.g., phytoplankton) since lidar is a more collimated light source with respect to the sun. Thus, a greater fraction of target-reflected/medium-reflected photons occur especially when particles are larger. This effect is expected to be more remarkable at shorter wavelengths (e.g., $< 450 \text{ nm}$) and may explain in part the absence of statistical R_{rs} - β relationships at 410 nm. At wavelengths longer than the FLOE laser wavelength, the R_{rs} - β linkage disappears as result of a smaller contribution of water-leaving photons in the red spectrum (i.e., $> 600 \text{ nm}$) due to the light absorption by water near the sea surface (1-2 m depth).

The greatest correlation between R_{rs} ratios and β parameters was found in the spectral range 490-508 nm. Within this spectral window, fish reflectivity is maximum and relatively constant¹⁷, thus we suggest that observed spectral differences on optical relationships were mainly accounted by particulate components other than fish and characterized by having a major influence on R_{rs} (blue light absorption by phytoplankton) and β (green light backscattering by zooplankton)¹⁸, and a mutual covariation for the spatial scale under study.

Our preliminary results encourage the analysis of spatial changes on R_{rs} ratios to detect sub-surface optical features such that drastic change on β -parameters at 12 m depth observed after bin # 175. The use of R_{rs} ratios to estimate some aspects of vertical distribution of lidar-derived optical properties need to be addressed with care since maximum depth range of correlation between R_{rs} ratios and β -parameters varied with wavelength and lidar backscattering property. Comparisons between shipboard optical profilers (e.g., PRR), airborne R_{rs} , and lidar backscattering parameters at multiple spatial scales (250 m to 9 km) are suggested in future studies to better understand vertical changes in optical properties based on above-water passive optical measurements.

4. REFERENCES

1. Carder K.L., R.G. Steward, "A remote-sensing reflectance model of a red tide dinoflagellate off west Florida", *Limnology and Oceanography* 30, 286-298, 1985.
2. Zanaveld JRV, "Remotely sensed reflectance and its dependence on vertical structure: a theoretical derivation", *Applied Optics*, 21, 4146-4150, 1982
3. Gordon H.R., O.B. Brown, "Diffuse reflectance of the ocean: some effects of vertical structure", *Applied Optics*, 14, 2892-2895, 1975.
4. Churnside J., P.L. Donaghay, "Thin scattering layers observed by airborne lidar", *ICES Journal of Marine Science*, 66, 778-789, 2009.
5. Montes-Hugo M., "Monte Carlo simulations as a tool to optimize target detection by AUV/ROV laser line scanners", Ms Sc thesis, USF, 84 p, 2005.
6. Churnside JH, J.J. Wilson, V.V. Tatarskii, "Airborne lidar for fisheries applications", *Optical Engineering*, 40, 406-414, 2001.
7. Fiorani L., I.G. Okladnikov, A. Palucci, "Lidar-calibrated regional models for satellite retrieval of primary productivity in the Southern Ocean", *Journal of Optoelectronics and Advanced Materials* 9, 3939-3945, 2007.
8. Powell K.A., C.A. Hostetler, Z. Liu, M. A. Vaughan, R.E. Kuehn, W.H. Hunt, K.P. Lee, C.R. Trepte, R. Rogers, S.A. Young, D.M. Winker, "CALIPSO Lidar Calibration Algorithms: Part I – Nighttime 532-nm Parallel Channel and 532-nm Perpendicular Channel", *Journal of Atmospheric and Oceanic Technology*, DOI: 10.1175/2009JTECHA1242.1, 2009.
9. Vaughan M., S. Young, D. Winker, K. Powell, A. Omar, Z. Liu, Y. Hu, C. Hostetler, "Fully automated analysis of space-based lidar data: an overview of the CALIPSO retrieval algorithms and data products", *SPIE Proceedings*, 5575, 16-30, 2004.
10. Gordon, H. R., D.K. Clark, J.W. Brown, O.B. Brown, R.H. Evans, W.W. Broenkow, "Phytoplankton pigment concentrations in the middle Atlantic bight: Comparisons between ship determinations and coastal zone color scanner estimates", *Applied Optics*, 22, 20-36, 1983.
11. Lee, Z., K.L. Carder, R.F. Chen, T.G. Peacock, "Properties of the water column and bottom derived from Airborne Visible Infrared Imaging Spectrometer (AVIRIS) data", *Journal of Geophysical Research*, 106, 11639-11651, 2001.
12. Montes-Hugo M., K. Carder, R. Foy, J. Cannizzaro, E. Brown, S. Pegau, "Estimating phytoplankton biomass in coastal waters of Alaska using airborne remote sensing", *Remote Sensing of Environment*, 98, 481-493, 2005.
13. Gordon H.R., O.B. Brown, R.E. Evans, J.W. Brown, R.C. Smith, K.S. Baker, D.C. Clark, "A semi-analytic model of ocean color", *Journal of Geophysical Research*, 93, 10909, 1988.
14. Churnside J.H., V. V. Tatarskii, J.J. Wilson, "Oceanographic Lidar Attenuation Coefficients and Signal Fluctuations Measured from a Ship in the Southern California Bight", *Applied Optics* 37, 3105-3112, 1998.
15. Churnside J.H., J.J. Wilson, V.V. Tatarskii, "Lidar profiles of fish schools", *Applied Optics* 36, 6011-6020, 1997.
16. Gordon H. R., A.Y. Morel, "Remote assessment of ocean color for interpretation of satellite visible imagery: A review", pp. 114, New York, Springer-Verlag press, 1983.
17. Lythgoe J.N., J. Shand, "Changes in spectral reflexions from iridophores of the neon tetra", *Journal of Physiology*, 325, 23-24, 1982.
18. Brown E.D, J.H. Churnside, R.L. Collins, T. Veenstra, J.J. Wilson, K. Abnctt, "Remote sensing of capelin and other biological features in the North Pacific using Lidar and video technology", *ICES Journal of Marine Science*, 59, 1120-1130, 2002.